Understanding the Capabilities of the HoloLens 1 and 2 in a Mixed Reality Environment for Direct Volume Rendering with a Ray-casting Algorithm

Hoijoon Jung*
University of Sydney, Australia

Younhyun Jung†
Gachon University, Republic of Korea

Jinman Kim‡
University of Sydney, Australia

2022 IEEE Conference on Virtual Reality and 3D User Interfaces Abstracts and Workshops (VRW) | 978-1-6654-8402-2/22/$31.00 ©2022 IEEE | DOI: 10.1109/VRW55335.2022.00200

ABSTRACT

Direct volume rendering (DVR) is a standard technique for visualizing scientific volumetric data in three-dimension (3D). Utilizing current mixed reality head-mounted displays (MR-HMDs), the DVR can be displayed as a 3D hologram that can be superimposed on the original 'physical' object, offering supplementary x-ray visions showing its interior features. These MR-MHDs are stimulating innovations in a range of scientific application fields, yet their capabilities on DVR have yet to be thoroughly investigated. In this study, we explore a key requirement of rendering latency capability for MR-HMDs by proposing a benchmark application with 5 volumes and 30 rendering parameter variations.

Index Terms: Computing methodologies—Computer graphics—Graphics systems and interfaces—Mixed / augmented reality; General and reference—Cross-computing tools and techniques—Evaluation

1 INTRODUCTION

Direct volume rendering (DVR) is a standard technique to visualize the volumetric data (volume) in three-dimension (3D) by projecting all sampled voxels to a rendering plane. Users can observe an overview of internal features in the volume and intuitively perceive their spatial relationships with DVR. Mixed reality (MR) creates an environment where the user's physical environments and the virtual contents are combined. Using MR, the DVR can be presented as a 3D hologram superimposed on the original 'physical' object, providing additional information on its interior features while maintaining direct views (e.g., x-ray vision). This superimposition can aid in volume assimilation and improve user performance in scientific applications (e.g., medicine), such that the interior features are visible *in situ* with an immediate view of the physical environment [2]. Commercially affordable MR head-mounted displays (MR-HMDs), such as Microsoft HoloLens, are stimulating innovation in a variety of scientific applications by using the MR-HMDs' rendering capability for effective DVR visualization [3, 7].

It is crucial to maintain low rendering latency in MR to avoid negative effects and provide the best experience to the user [4]. Without timely rendering capability, DVR visualization would appear unstable, jittering, or 'swimming around' in the physical environment which would not be seen as precisely intermixed or augmented to the original object [1]. However, it is challenging to maintain low latency on MR-HMDs with DVR due to its high computational load. MR-HMDs have limited computational resources compared to their computer counterparts, such as desktops and laptops, due to their necessity to be wearable and portable, and their battery-dependent nature.

We contend that understanding the rendering capabilities of MR-HMDs, as well as the latency, can play a fundamental role in the acceptance of MR-based DVR in scientific applications. However, there is a scarcity of studies into the rendering capabilities of commercially available MR-HMDs for DVR. Prior studies focused on determining the impact of MR-based DVR on user performance, e.g., accuracy and time spent on medical needle placement [3, 7], rather than evaluating the MR-HMD's capabilities to create practical rendering latency for various scientific applications.

This study investigates the rendering capabilities of two commercial MR-HMDs from different generations, HoloLens 1 (HL1) and HoloLens 2 (HL2), for DVR visualization using our proposing benchmarking application with 5 volumes and 30 rendering parameter variations.

*e-mail: hoijoon.jung@sydney.edu.au
†e-mail: younhyun.jung@gachon.ac.kr
‡e-mail: jinman.kim@sydney.edu.au

2 METHOD

Figure 1 depicts the evaluation process, showing how the inputs (transfer function, volumes, and rendering parameters) are fed into the proposing benchmarking application, which then produces the outputs (i.e., DVR visualization and its rendering latency). Our benchmarking application is a custom implementation using Unity 2018.4 and MR toolkit (MRTK) V2.3.0 and consists of a Single-pass raycasting DVR pipeline, automatic benchmarking mechanism, and Unity profiler.

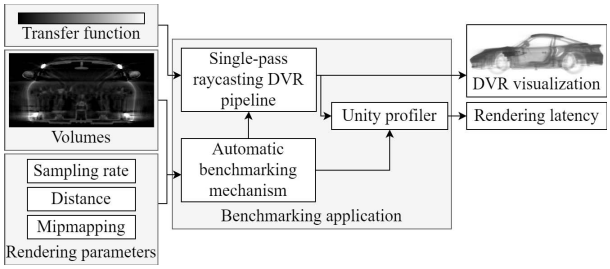

Figure 1: Overview of the evaluation process

The evaluation employed 5 volumes [6, 8] as listed in Table 1. Three rendering parameters: sampling rate, rendering distance (between DVR visualization and user), and mipmapping were used for producing 30 rendering parameter variations: 5 sampling rates (0.0625, 0.125, 0.25. 0.5 and 1) × 3 rendering distances (1.5m, 2m and 2.5m) × 2 mipmapping (on and off). On each of HL1 and 2, 150 DVR visualizations (5 volumes × 30 rendering parameter variations) were evaluated.

The rendering latency of each DVR visualization on each HL was acquired from 100 rendering frames while the volume was randomly rotating. In total, 30,000 records of rendering latency (150 DVR visualizations × 100 rendering frames × 2 MR-HMDs) were obtained. Due to the application close caused by HL2's operating system, 300 records of rendering latency from Porsche volume on HL2 with a sampling rate of 1 and mipmapping off were discarded. The average rendering latency (lower is better) was calculated and categorized according to the recommendations of MR-HMD vendors [5]: optimal ($\leq$16.7 milliseconds (ms)), practical (16.7 – 22.2 ms), minimal (22.2 – 33.3 ms), and impractical ($\geq$33.3 ms).

978-1-6654-8402-2/22/$31.00 ©2022 IEEE
DOI 10.1109/VRW55335.2022.00200

Table 1: 5 volumes with resolution in voxel (Width×Height×Depth), bit depth in bits, data size in megabytes, and physical size in centimeter (Width×Height×Depth).

Volume	Resolution	Bit depth	Data size	Physical size
Bonsai	512×512×189	16	94.5	20.6×20.6×18.9
Human-CT	512×512×226	16	113.0	50×50×67.8
Clouds	512×512×32	8	8.0	51.2×51.2×3.2
Engine	256×256×256	8	16.0	25.6×25.6×25.6
Porsche	559×1023×347	8	189.2	55.9×102.3×34.7

3 Results

The average rendering latency of DVR visualizations on HL1 and HL2 is categorized in Table 2. Overall, the DVR visualizations on HL2 showed improved average rendering latency than those on HL1, where HL2 had 43 additional DVR visualizations that resulted in the optimal, practical, or minimal categories over HL1 (see Figure 2). In terms of the distribution ratio of the categories, HL2 had an increased distribution ratio in the optimal category which was increased by 29.4%, and the increase in the practical category was 1.5%. In other words, a smaller number of DVR visualizations was distributed to the minimal (-1.1%) and impractical (-29.7%) categories on HL2.

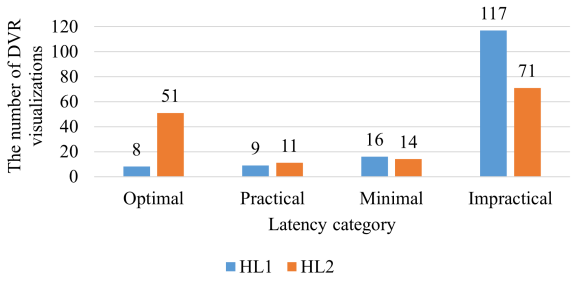

Figure 2: The result of average rendering latency grouped by MR-HMD and latency categories

DVR visualizations in HL1 and HL2 showed varying average rendering latency with different volumes. The volumes with lower resolution tend to show better average rendering latency. Mipmapping improved the average rendering latency on both the HL1 and HL2 where a larger number of DVR visualizations were categorized into optimal, practical, or minimal categories than without it. The sampling rate had a positive correlation with the average rendering latency on HL1 and HL2 where fewer DVR visualizations resulted in optimal, practical, or minimal categories with higher sampling rates. On the other hand, the rendering distance had a negative correlation with the average rendering latency on HL1 and HL2.

4 Conclusion

This preliminary study found that when mipmapping is enabled, HL2 is a viable MR-HMD to enable interactive DVR visualization with a volume that has a standard volume resolution. For volumes with higher resolutions, it is recommended to downscale the volume's physical size so that the DVR display size can be reduced and ease the DVR calculation. As expected, the newer generation, HL2, outperformed HL1, but HL1 is still valuable in visualizing volumes with low resolution. For producing practical rendering latency while maintaining the volume's original physical size, different DVR optimization algorithms, e.g., dynamically adjusting sampling rate based on rendering latency, would be investigated and optimized with MR-HMDs.

Table 2: Average rendering latency of DVR visualizations categorized in optimal (O), practical (P), minimal (M), and impractical (I) colored in green, blue, yellow, and red, respectively, and presented in HL1/HL2. Note that Vol. refers to Volume and Mipmap. refers to Mipmapping.

Vol.	Mipmap.	Distance	Sampling Rate 0.0625	0.125	0.25	0.5	1
Bonsai	Off	1.5	M/M	I/I	I/I	I/I	I/I
		2	M/M	I/I	I/I	I/I	I/I
		2.5	M/M	I/I	I/I	I/I	I/I
	On	1.5	P/O	M/O	I/O	I/P	I/M
		2	O/O	P/O	M/O	I/O	I/P
		2.5	O/O	O/O	M/O	I/O	I/O
Human-CT	Off	1.5	I/I	I/I	I/I	I/I	I/I
		2	I/I	I/I	I/I	I/I	I/I
		2.5	I/I	I/I	I/I	I/I	I/I
	On	1.5	I/I	I/I	I/I	I/I	I/I
		2	I/M	I/I	I/I	I/I	I/I
		2.5	I/P	I/M	I/I	I/I	I/I
Clouds	Off	1.5	I/O	I/O	I/P	I/I	I/I
		2	M/O	I/O	I/O	I/M	I/I
		2.5	P/O	M/O	I/O	I/P	I/M
	On	1.5	I/O	I/O	I/P	I/I	I/I
		2	M/O	I/O	I/O	I/P	I/M
		2.5	P/O	M/O	I/O	I/O	I/M
Engine	Off	1.5	P/O	M/O	I/O	I/P	I/I
		2	O/O	P/O	M/O	I/P	I/M
		2.5	O/O	P/O	M/O	I/O	I/M
	On	1.5	P/O	M/O	I/O	I/P	I/M
		2	O/O	P/O	M/O	I/O	I/P
		2.5	O/O	O/O	M/O	I/O	I/O
Porsche	Off	1.5	I/I	I/I	I/I	I/I	I/-
		2	I/I	I/I	I/I	I/I	I/-
		2.5	I/I	I/I	I/I	I/I	I/-
	On	1.5	I/I	I/I	I/I	I/I	I/I
		2	I/I	I/I	I/I	I/I	I/I
		2.5	I/M	I/I	I/I	I/I	I/I

References

[1] J. Carmigniani, B. Furht, M. Anisetti, P. Ceravolo, E. Damiani, and M. Ivkovic. Augmented reality technologies, systems and applications. *Multimed. Tools Appl.*, 51(1):341–377, 2011.

[2] L. Chen, T. W. Day, W. Tang, and N. W. John. Recent developments and future challenges in medical mixed reality. In *IEEE international symposium on mixed and augmented reality*, pp. 123–135. IEEE, 2017.

[3] J. Gibby, S. Cvetko, R. Javan, R. Parr, and W. Gibby. Use of augmented reality for image-guided spine procedures. *Eur. Spine J.*, 29(8):1823–1832, 2020.

[4] K. Kim, M. Billinghurst, G. Bruder, H. B.-L. Duh, and G. F. Welch. Revisiting trends in augmented reality research: A review of the 2nd decade of ismar (2008–2017). *IEEE Trans. Vis. Comput. Graph.*, 24(11):2947–2962, 2018.

[5] Microsoft. Hologram stability. https://docs.microsoft.com/en-us/windows/mixed-reality/develop/advanced-concepts/hologram-stability (Accessed: 20 Sep. 2020).

[6] OsiriX. Dicom image library. https://www.osirix-viewer.com/resources/dicom-image-library/ (Accessed: 10 Jun. 2021).

[7] B. J. Park, S. J. Hunt, C. Martin III, G. J. Nadolski, B. J. Wood, and T. P. Gade. Augmented and mixed reality: technologies for enhancing the future of ir. *J. Vasc. Interv. Radiol.*, 31(7):1074–1082, 2020.

[8] S. Roettger. The volume library. http://schorsch.efi.fh-nuernberg.de/data/volume (Accessed: 10 Jun. 2021).